Validation of diffuse correlation spectroscopy for muscle blood flow with concurrent arterial spin labeled perfusion MRI

Guoqiang Yu[1], Thomas F. Floyd[2], Turgut Durduran[1, 3], Chao Zhou[1], Jiongjiong Wang[3], John A. Detre[3], Arjun G. Yodh[1]

[1]Department of Physics and Astronomy, [2]Departments of Anesthesiology, [3]Center for Functional Neuroimaging, Department of Radiology, University of Pennsylvania, Philadelphia, PA 19104
guoqiang@physics.upenn.edu

Abstract: Calf blood flow was measured simultaneously in healthy human subjects (n = 7) during cuff inflation and deflation using near-infrared diffuse correlation spectroscopy (DCS) and arterial spin labeled perfusion MRI (ASL-MRI). The DCS and ASL-MRI data exhibited highly correlated absolute and relative dynamic flow responses in each individual ($p < 0.001$). Peak flow variations during hyperemia were also significantly correlated, though more for relative ($p = 0.003$) than absolute ($p = 0.016$) flow. Repeated measurement variation was less than 8% for both modalities. The results provide much needed quantitative blood flow validation of the diffuse optical correlation method in humans.

OCIS codes: (170.0170) Medical optics and biotechnology; (170.3880) Medical and biological imaging; (170.6480) Spectroscopy, speckle; (170.3660) Light propagation in tissues.

References and links

1. U. Wolf, M. Wolf, J. H. Choi, M. Levi, D. Choudhury, S. Hull, D. Coussirat, L. A. Paunescu, L. P. Safonova, A. Michalos, W. W. Mantulin, and E. Gratton, "Localized irregularities in hemoglobin flow and oxygenation in calf muscle in patients with peripheral vascular disease detected with near-infrared spectrophotometry," J. Vasc. Surg. **37**, 1017-1026 (2003).
2. T. Binzoni, T. S. Leung, D. Boggett, and D. Delpy, "Non-invasive laser Doppler perfusion measurements of large tissue volumes and human skeletal muscle blood RMS velocity," Phys. Med. Biol. **48**, 2527-2549 (2003).
3. T. Binzoni, T. S. Leung, D. Rufenacht, and D. T. Delpy, "Absorption and scattering coefficient dependence of laser-Doppler flowmetry models for large tissue volumes," Phys. Med. Biol. **51**, 311-333 (2006).
4. R. J. Whitney, "The measurement of volume changes in human limbs," J. Physiol. **121**, 1-27 (1953).
5. E. Keller, A. Nadler, H. Alkadhi, S. S. Kollias, Y. Yonekawa, and P. Niederer, "Noninvasive measurement of regional cerebral blood flow and regional cerebral blood volume by near-infrared spectroscopy and indocyanine green dye dilution," Neuroimage **20**, 828-839 (2003).
6. W. Burchert, S. Schellong, J. van den Hoff, G. J. Meyer, K. Alexander, and H. Hundeshagen, "Oxygen-15-water PET assessment of muscular blood flow in peripheral vascular disease," J. Nucl. Med. **38**, 93-98 (1997).
7. K. A. Engelke, J. R. Halliwill, D. N. Proctor, N. M. Dietz, and M. J. Joyner, "Contribution of nitric oxide and prostaglandins to reactive hyperemia in human forearm," J. Appl. Physiol. **81**, 1807-1814 (1996).
8. J. R. Libonati, A. K. Howell, N. M. Incanno, K. K. Pettee, and H. L. Glassberg, "Brief muscle hypoperfusion/hyperemia: an ergogenic aid?," J. Strength. Cond. Res. **15**, 362-366 (2001).
9. J. R. Libonati, M. Cox, N. Incanno, S. K. Melville, F. C. Musante, H. L. Glassberg, and M. Guazzi, "Brief periods of occlusion and reperfusion increase skeletal muscle force output in humans," Cardiologia **43**, 1355-1360 (1998).
10. R. Joannides, W. E. Haefeli, L. Linder, V. Richard, E. H. Bakkali, C. Thuillez, and T. F. Luscher, "Nitric oxide is responsible for flow-dependent dilatation of human peripheral conduit arteries in vivo," Circulation **91**, 1314-1319 (1995).
11. C. Binggeli, L. E. Spieker, R. Corti, I. Sudano, V. Stojanovic, D. Hayoz, T. F. Luscher, and G. Noll, "Statins enhance postischemic hyperemia in the skin circulation of hypercholesterolemic patients: a monitoring test of endothelial dysfunction for clinical practice?," J. Am. Coll. Cardiol. **42**, 71-77 (2003).
12. J. A. Detre, J. S. Leigh, D. S. Williams, and A. P. Koretsky, "Perfusion imaging," Magn. Reson. Med. **23**, 37-45 (1992).

#76741 - $15.00 USD Received 3 November 2006; revised 14 January 2007; accepted 16 January 2007

13. D. S. Williams, J. A. Detre, J. S. Leigh, and A. P. Koretsky, "Magnetic resonance imaging of perfusion using spin inversion of arterial water," Proc. Natl. Acad. Sci. U.S.A. **89**, 212-216 (1992).
14. J. S. Raynaud, S. Duteil, J. T. Vaughan, F. Hennel, C. Wary, A. Leroy-Willig, and P. G. Carlier, "Determination of skeletal muscle perfusion using arterial spin labeling NMRI: validation by comparison with venous occlusion plethysmography," Magn. Reson. Med. **46**, 305-311 (2001).
15. V. Lebon, P. G. Carlier, C. Brillault-Salvat, and A. Leroy-Willig, "Simultaneous measurement of perfusion and oxygenation changes using a multiple gradient-echo sequence: application to human muscle study," Magn. Reson. Imaging **16**, 721-729 (1998).
16. B. Siewert, G. Schlaug, R. R. Edelman, and S. Warach, "Comparison of EPISTAR and T2*-weighted gadolinium-enhanced perfusion imaging in patients with acute cerebral ischemia," Neurology **48**, 673-679 (1997).
17. M. A. Weber, M. Gunther, M. P. Lichy, S. Delorme, A. Bongers, C. Thilmann, M. Essig, I. Zuna, L. R. Schad, J. Debus, and H. P. Schlemmer, "Comparison of arterial spin-labeling techniques and dynamic susceptibility-weighted contrast-enhanced MRI in perfusion imaging of normal brain tissue," Invest. Radiol. **38**, 712-718 (2003).
18. R. L. Wolf, D. C. Alsop, M. L. McGarvey, J. A. Maldjian, J. Wang, and J. A. Detre, "Susceptibility contrast and arterial spin labeled perfusion MRI in cerebrovascular disease," J. Neuroimaging **13**, 17-27 (2003).
19. D. A. Boas, L. E. Campbell, and A. G. Yodh, "Scattering and Imaging with Diffusing Temporal Field Correlations," Phys. Rev. Lett. **75**, 1855-1858 (1995).
20. D. A. Boas and A. G. Yodh, "Spatially varying dynamical properties of turbid media probed with diffusing temporal light correlation," J. Opt. Soc. Am. A **14**, 192-215 (1997).
21. T. Durduran, G. Yu, M. G. Burnett, J. A. Detre, J. H. Greenberg, J. Wang, C. Zhou, and A. G. Yodh, "Diffuse optical measurement of blood flow, blood oxygenation, and metabolism in a human brain during sensorimotor cortex activation," Opt. Lett. **29**, 1766-1768 (2004).
22. J. P. Culver, T. Durduran, D. Furuya, C. Cheung, J. H. Greenberg, and A. G. Yodh, "Diffuse optical tomography of cerebral blood flow, oxygenation, and metabolism in rat during focal ischemia," J Cereb. Blood Flow Metab. **23**, 911-924 (2003).
23. C. Cheung, J. P. Culver, K. Takahashi, J. H. Greenberg, and A. G. Yodh, "In vivo cerebrovascular measurement combining diffuse near-infrared absorption and correlation spectroscopies," Phys. Med. Biol. **46**, 2053-2065 (2001).
24. J. Li, G. Dietsche, D. Iftime, S. E. Skipetrov, G. Maret, T. Elbert, B. Rockstroh, and T. Gisler, "Noninvasive detection of functional brain activity with near-infrared diffusing-wave spectroscopy," J. Biomed. Opt. **10**, 044002 (2005).
25. C. Zhou, G. Q. Yu, D. Furuya, J. H. Greenberg, A. G. Yodh, and T. Durduran, "Diffuse optical correlation tomography of cerebral blood flow during cortical spreading depression in rat brain," Opt. Express **14**, 1125-1144 (2006).
26. G. Yu, T. Durduran, H. W. Wang, C. Zhou, E. M. Putt, H. M. Saunders, C. M. Sehgal, E. Glatstein, A. G. Yodh, and T. M. Busch, "Noninvasive Monitoring of Murine Tumor Blood Flow During and After Photodynamic Therapy Provides Early Assessment of Therapeutic Efficacy," Clin. Cancer Res. **11**, 3543-3552 (2005).
27. G. Yu, T. Durduran, C. Zhou, T. C. Zhu, J. C. Finlay, T. M. Busch, S. B. Malkowicz, S. M. Hahn, and A. G. Yodh, "Real-time In Situ Monitoring of Human Prostate Photodynamic Therapy with Diffuse Light," Photochem. Photobiol. **82**, 1279-1284 (2006).
28. T. Durduran, R. Choe, G. Yu, C. Zhou, J. C. Tchou, B. J. Czerniecki, and A. G. Yodh, "Diffuse optical measurement of blood flow in breast tumors," Opt. Lett. **30**, 2915-2917 (2005).
29. U. Sunar, H. Quon, T. Durduran, J. Zhang, J. Du, C. Zhou, G. Yu, R. Choe, A. Kilger, R. Lustig, L. Loevner, S. Nioka, B. Chance, and Y. A. G., "Non-invasive diffuse optical measurement of blood flow and blood oxygenation for monitoring radiation therapy in patients with head and neck tumors," J. Biomed. Opt. **11,** 064021 (2006).
30. G. Yu, T. Durduran, G. Lech, C. Zhou, B. Chance, E. R. Mohler, and A. G. Yodh, "Time-dependent Blood Flow and Oxygenation in Human Skeletal Muscles Measured with Noninvasive Near-infrared Diffuse Optical Spectroscopies," J. Biomed. Opt. **10**, 024027 (2005).
31. E. G. Walsh, K. Minematsu, J. Leppo, and S. C. Moore, "Radioactive microsphere validation of a volume localized continuous saturation perfusion measurement," Magn. Reson. Med. **31**, 147-153 (1994).
32. G. S. Pell, M. D. King, E. Proctor, D. L. Thomas, M. F. Lythgoe, D. G. Gadian, and R. J. Ordidge, "Comparative study of the FAIR technique of perfusion quantification with the hydrogen clearance method," J. Cereb. Blood Flow Metab. **23**, 689-699 (2003).
33. D. S. Williams, D. J. Grandis, W. Zhang, and A. P. Koretsky, "Magnetic resonance imaging of perfusion in the isolated rat heart using spin inversion of arterial water," Magn. Reson. Med. **30**, 361-365 (1993).
34. F. Q. Ye, K. F. Berman, T. Ellmore, G. Esposito, J. D. van Horn, Y. Yang, J. Duyn, A. M. Smith, J. A. Frank, D. R. Weinberger, and A. C. McLaughlin, "H(2)(15)O PET validation of steady-state arterial spin tagging cerebral blood flow measurements in humans," Magn. Reson. Med. **44**, 450-456 (2000).
35. C. M. Feng, S. Narayana, J. L. Lancaster, P. A. Jerabek, T. L. Arnow, F. Zhu, L. H. Tan, P. T. Fox, and J. H. Gao, "CBF changes during brain activation: fMRI vs. PET," Neuroimage **22**, 443-446 (2004).
36. T. F. Floyd, S. J. Ratcliffe, J. Wang, B. Resch, and J. A. Detre, "Precision of the CASL-perfusion MRI technique for the measurement of cerebral blood flow in whole brain and vascular territories," J. Magn. Reson. Imaging **18**, 649-655 (2003).
37. J. Wang, G. K. Aguirre, D. Y. Kimberg, A. C. Roc, L. Li, and J. A. Detre, "Arterial spin labeling perfusion fMRI with very low task frequency," Magn. Reson. Med. **49**, 796-802 (2003).

#76741 - $15.00 USD Received 3 November 2006; revised 14 January 2007; accepted 16 January 2007

38. Y. F. Yen, A. S. Field, E. M. Martin, N. Ari, J. H. Burdette, D. M. Moody, and A. M. Takahashi, "Test-retest reproducibility of quantitative CBF measurements using FAIR perfusion MRI and acetazolamide challenge," Magn. Reson. Med. **47**, 921-928 (2002).
39. L. M. Parkes, W. Rashid, D. T. Chard, and P. S. Tofts, "Normal cerebral perfusion measurements using arterial spin labeling: reproducibility, stability, and age and gender effects," Magn. Reson. Med. **51**, 736-743 (2004).
40. D. J. Pine, D. A. Weitz, P. M. Chaikin, and Herbolzheimer, "Diffusing-wave spectroscopy," Phys. Rev. Lett. **60**, 1134-1137 (1988).
41. G. Maret and P. E. Wolf, "Multiple light scattering from disordered media. The effect of Brownian motion of scatterers," Z. Phys. B **65**, 409-413 (1987).
42. Heckmeier, S. E. Skipetrov, G. Maret, and R. Maynard, "Imaging of dynamic heterogeneities in multiple-scattering media," J. Opt. Soc. Am. A **14**, 185-191 (1997).
43. D. A. Boas, "Diffuse Photon Probes of Structural and Dynamical Properties of Turbid Media: Theory and Biomedical Applications," Ph.D. Dissertation (University of Pennsylvania, Philadelphia, 1996).
44. A. Einstein, "On the motion of small particles suspended in liquids at rest required by the molecular-kinetic theory of heat," Annalen. der. Physik **17**, 549-560 (1905).
45. L. R. Frank, E. C. Wong, L. J. Haseler, and R. B. Buxton, "Dynamic imaging of perfusion in human skeletal muscle during exercise with arterial spin labeling," Magn. Reson. Med. **42**, 258-267 (1999).
46. J. Wang, Y. Zhang, R. L. Wolf, A. C. Roc, D. C. Alsop, and J. A. Detre, "Amplitude-modulated continuous arterial spin-labeling 3.0-T perfusion MR imaging with a single coil: feasibility study," Radiology **235**, 218-228 (2005).
47. T. F. Floyd, J. Wang, J. M. Murphy, N. S. Butler, and J. A. Detre, "Feasibility of the application of CASL for the diagnosis of peripheral vascular disease," presented at the Proc. Intl. Soc. Magn. Reson. Med., 2005.
48. G. K. Aguirre, J. A. Detre, E. Zarahn, and D. C. Alsop, "Experimental design and the relative sensitivity of BOLD and perfusion fMRI," Neuroimage **15**, 488-500 (2002).
49. D. C. Alsop and J. A. Detre, "Multisection cerebral blood flow MR imaging with continuous arterial spin labeling," Radiology **208**, 410-416 (1998).
50. E. T. Petersen, I. Zimine, Y. C. Ho, and X. Golay, "Non-invasive measurement of perfusion: a critical review of arterial spin labelling techniques," Br. J. Radiol. **79**, 688-701 (2006).
51. J. F. Toussaint, K. K. Kwong, F. O. Mkparu, R. M. Weisskoff, P. J. LaRaia, H. L. Kantor, and F. M'Kparu, "Perfusion changes in human skeletal muscle during reactive hyperemia measured by echo-planar imaging," Magn. Reson. Med. **35**, 62-69 (1996).
52. J. F. Toussaint, K. K. Kwong, F. M'Kparu, R. M. Weisskoff, P. J. LaRaia, and H. L. Kantor, "Interrelationship of oxidative metabolism and local perfusion demonstrated by NMR in human skeletal muscle," J. Appl. Physiol. **81**, 2221-2228 (1996).
53. H. Lu, M. J. Donahue, and P. C. van Zijl, "Detrimental effects of BOLD signal in arterial spin labeling fMRI at high field strength," Magn. Reson. Med. **56**, 546-552 (2006).
54. C. W. Song, "Effect of local hyperthermia on blood flow and microenvironment: a review," Cancer Res. **44**, 4721s-4730s (1984).
55. A. G. Sorensen, W. A. Copen, L. Ostergaard, F. S. Buonanno, R. G. Gonzalez, G. Rordorf, B. R. Rosen, L. H. Schwamm, R. M. Weisskoff, and W. J. Koroshetz, "Hyperacute stroke: simultaneous measurement of relative cerebral blood volume, relative cerebral blood flow, and mean tissue transit time," Radiology **210**, 519-527 (1999).
56. B. W. Pogue, R. D. Braun, J. L. Lanzen, C. Erickson, and M. W. Dewhirst, "Analysis of the heterogeneity of pO2 dynamics during photodynamic therapy with verteporfin," Photochem. Photobiol. **74**, 700-706 (2001).
57. C. A. Mack, C. J. Magovern, K. T. Budenbender, S. R. Patel, E. A. Schwarz, P. Zanzonico, B. Ferris, T. Sanborn, P. Isom, O. W. Isom, R. G. Crystal, and T. K. Rosengart, "Salvage angiogenesis induced by adenovirus-mediated gene transfer of vascular endothelial growth factor protects against ischemic vascular occlusion," J. Vasc. Surg. **27**, 699-709 (1998).
58. V. Quaresima, M. Ferrari, M. A. Franceschini, M. L. Hoimes, and S. Fantini, "Spatial distribution of vastus lateralis blood flow and oxyhemoglobin saturation measured at the end of isometric quadriceps contraction by multichannel near-infrared spectroscopy," J. Biomed. Opt. **9**, 413420 (2004).

1. Introduction

Although a variety of methods for assessment of tissue blood flow have been explored [1-13], it has been difficult to continuously measure local muscle blood flow in humans non-invasively and directly. Conventional venous occlusion plethysmography measures limb blood flow when venous outflow is occluded based on the volume increase with time in a limb segment [4, 7]. This method, however, does not provide regional and continuous information and can be used only in the static state or during brief exercise, since venous occlusion interrupts blood flow. Doppler ultrasound is a common clinical tool but is limited to measurement of blood flow within large vessels [8, 9]. Laser Doppler Flowmetry (LDF) is used primarily for non-invasive and continuous monitoring of the skin perfusion [10, 11],

#76741 - $15.00 USD Received 3 November 2006; revised 14 January 2007; accepted 16 January 2007

although recently Binzoni *et al* have extended its application to relatively deeper tissues (~0.5 cm below tissue surface) [2]. Arterial spin labeled perfusion magnetic resonance imaging (ASL-MRI) [12-15] and dynamic contrast agent MRI [16-18] provide perfusion images with high spatial resolution; however, their clinical use is limited due to high cost, low throughput and low mobility. Positron emission tomography (PET) [6] has similar clinical limitations with decreased spatial resolution compared to MRI.

Near-infrared diffuse correlation spectroscopy (DCS) [19, 20] is an emerging technique for non-invasive measurement of blood flow in deep tissues. It enables continuous measurements of blood flow with high temporal (~100 ms) and limited spatial (~1 mm) resolution in tissue. DCS has been applied for the investigation of cerebral hemodynamics [21-25], photodynamic therapy [26, 27], cancers [28, 29], and muscle physiology [30]. Measurements of blood flow by DCS have been validated semi-quantitatively with color-weighted power Doppler Ultrasound in mouse tumors [26] and with laser Doppler in rat brain [22, 23]. Although these experiments suggest DCS is sensitive to microvascular flow, the method has not been directly compared to a validated approach in humans, and widespread clinical acceptance of the diffuse optical flow technique requires validation.

The primary objective of this study was to validate DCS tissue blood flow measurements in humans by comparison with a relatively established flow imaging modality: arterial spin labeled perfusion MRI (ASL-MRI). Utilizing magnetically labeled arterial blood water as an endogenous tracer, the ASL-MRI method has been shown to provide quantitative measurement of tissue perfusion in "classical" units of (ml/min)/100g-tissue [12, 13]. Note, herein we will use the term "tissue blood flow" interchangeably with "tissue perfusion".

Validation studies of ASL-MRI against other modalities in animal models have included comparisons with microspheres [31], hydrogen clearance [32], and flowmeters [33]. Cerebral blood flow (CBF) measurements with ASL-MRI have been shown to agree with results from $H_2{}^{15}O$-PET in humans at rest [34] and during functional activation [35], and with the dynamic susceptibility contrast agent approach [16-18]. ASL-MRI CBF measurements both at rest and during task activation have been demonstrated to be highly reproducible over time intervals ranging from a few minutes to several days [36-39], and the ASL-MRI measurement has been validated in skeletal muscle by comparison with venous occlusion plethysmography [14].

For validation purposes, it is desirable to compare the flow responses measured by the two techniques in the same tissue region. Therefore, in the present investigation calf muscle blood flow was concurrently measured by DCS and ASL-MRI during a reactive paradigm. The MRI measurement also provided anatomic information for accurate co-registration of the optical and MRI measurements. To the best of our knowledge, these explorations are the first *concurrent* clinical measurements of *blood flow* in human skeletal muscles using optical and MRI techniques, as well as the first direct validation of DCS blood flow in humans.

2. Materials and methods

2.1 Experimental configuration and protocols

Seven male healthy volunteers (ages 25–42) participated in the study with IRB approval and appropriate consent. Figure 1 shows a schematic of the measurement configuration. The volunteers were positioned supine and a custom-designed nonmagnetic optical probe for the DCS measurement was placed over the calf and secured with an elastic bandage. Flexible silicone material was used to tightly hold source and detector fibers in place. The calf (with the optical probe) was then placed into the MRI knee coil. The optical probe in the MRI room was connected to the DCS instrument in the control room by optical fibers through a port in a magnetic-field-shielded wall (see Fig. 1).

The accuracy and reliability of the ASL-MRI measurement is limited when muscle blood flow is low [14], e.g. in the resting state. Therefore we employed a cuff inflation paradigm to create a brief period of ischemia and hyperemic response. A nonmagnetic cuff was placed on the thigh, and connected to a tourniquet machine (Zimmer ATS 1000, Soma Technology, Inc., OH) in order to induce cuff inflation. A five-minute cuff inflation paradigm was tested: 2-

#76741 - $15.00 USD Received 3 November 2006; revised 14 January 2007; accepted 16 January 2007

minute baseline → 5-minute cuff inflation (250 mmHg) → 5-minute deflation. This paradigm was carried out twice on three volunteers to assess repeatability. MRI image slice and DCS probe position were marked to facilitate repeated data acquisition from the same location. In addition to the primary validation study on seven subjects (n = 7), the influence of probe pressure on muscle blood flow was tested; ASL-MRI data following cuff inflation were compared under two measurement conditions: (1) No optical probe (n = 4), and (2) wrapped probe on leg with elastic bandage (n = 4). Table 1 summarizes the measurements.

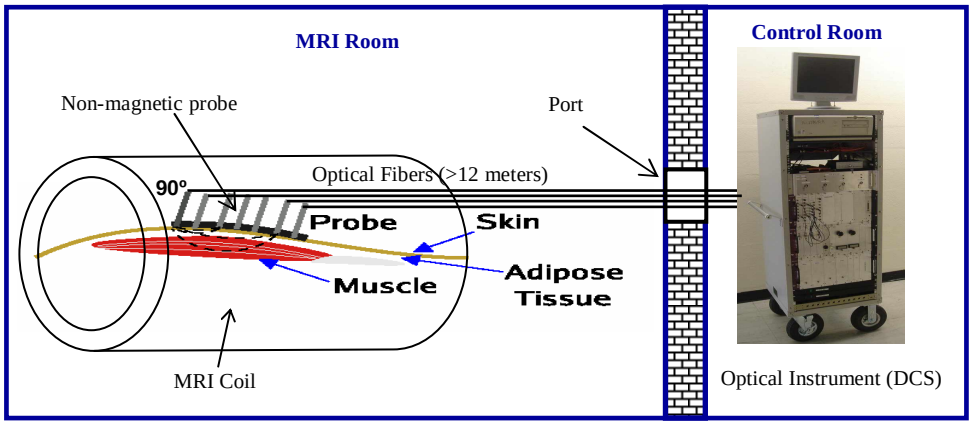

Fig. 1. Schematic of the concurrent optical-MRI measurement. A custom-designed nonmagnetic fiber-optic probe (see Fig. 2(d)) was placed over the calf. The tips of source and detector fibers were bent 90° and tightly held in place by flexible silicone material. The calf (with the optical probe) was then placed into the MRI knee coil. The optical probe in the MRI room was connected to the DCS instrument in the control room by 12-meter-length fibers through a port in a magnetic-field-shielded wall.

Table 1. Subject information and measurement summary. The thickness of the near-surface layer was measured from the MRI anatomic image. Concurrent optical-MRI measurements were repeated twice on three subjects (#1 to #3) to assess repeatability. In order to investigate the probe pressure influence on muscle blood flow, four subjects (#4 to #7) were measured with and without optical probe, respectively.

Subject #	Thickness (mm) of the near-surface layer (skin and adipose tissue)	Concurrent measurement DCS+ASL-MRI	ASL-MRI measurement only (without optical probe)
1	5.6	Repeat twice	
2	5.6	Repeat twice	
3	5.6	Repeat twice	
4	4.7	Once	Once
5	7.5	Once	Once
6	4.7	Once	Once
7	4.7	Once	Once
Mean	5.5		
STD	1.0		

#76741 - $15.00 USD Received 3 November 2006; revised 14 January 2007; accepted 16 January 2007

2.2 Diffuse correlation spectroscopy (DCS)

Details of the optical instrument for diffuse correlation spectroscopy are described elsewhere [30]. Briefly, a narrowband CW laser (785 nm, Crystalaser Inc., NV) with long coherence length (> 50 meter), four fast photon-counting, avalanche photodiodes (APD) (SPCM-AQR-14-FC, Pacer Components Inc., UK), and a four-channel autocorrelator board (Flex03OEM-4CH, Correlator Inc., NJ) facilitated measurements of blood flow. The light intensity fluctuations within a single speckle area are detected using a single mode fiber and an APD. The autocorrelator takes the APD output and uses photon arrival times to compute the light intensity autocorrelation function. From the normalized intensity autocorrelation function, we calculate the electric field temporal autocorrelation function $G_1(\mathbf{r},\tau)$, which satisfies the correlation diffusion equation in highly scattering media [19, 20, 40-42]. The correlation diffusion equation can have different forms depending on the nature and heterogeneity of the scatterer motion. For the important case of random ballistic flow in the tissue vasculature, the mean-square displacement, ($\langle\Delta\mathbf{r}^2(\tau)\rangle$), of the scattering particles (e.g. blood cells) in time τ is $\langle\Delta\mathbf{r}^2(\tau)\rangle = \langle V^2\rangle\tau^2$. Here $\langle V^2\rangle$ is the second moment of the cell speed distribution. For the case of diffusive motion, $\langle\Delta\mathbf{r}^2(\tau)\rangle = 6D_B\tau$, where D_B is an *effective* diffusion coefficient of the moving scatterers. We have found that the latter model very often provides better quality fits than the former model [23]. In this case the correlation function $G_1(\mathbf{r},\tau)$ will decay approximately exponentially in τ. Its decay rate, Γ (sec^{-1}), depends on a parameter α (proportional to the tissue blood volume fraction), and on the motion of the blood cells. A description of these concepts and approximations can be found in references [22, 23, 43].

The DCS measurement explicitly yields a blood flow-index αD_B [22, 23, 30]. The effective diffusion constant, D_B (cm^2/sec), differs from the traditional Stokes-Einstein diffusion coefficient [44], and α (unitless) represents the fraction of photon scattering events in the tissue from moving cells. Changes in this flow-index (αD_B) have been found to correlate well with other flow measurement modalities such as laser Doppler [22, 23] and color-weighted power Doppler Ultrasound [26]. The reported relative change of tissue blood flow, rBF, is derived from the relative change of αD_B, i.e. $rBF = \alpha D_B/(\alpha D_B)_{baseline}$. The utility of rBF has been demonstrated in several physiological contexts [21-24, 26, 29, 30].

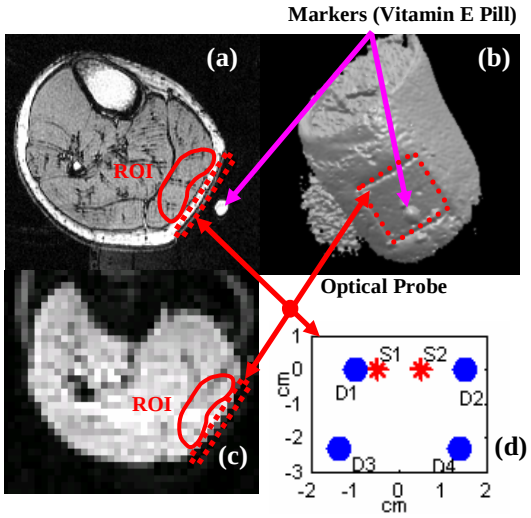

Fig. 2. MRI images (a, b, and c) obtained from one subject's calf. The optical probe and the MRI marker can be seen from 2-D (a) and 3-D (b) anatomic MRI images of human leg. The ASL-MRI perfusion image is shown in (c). The region of interest (ROI) shown in (a) and (c) was selected for the comparison of tissue responses measured by DCS and ASL-MRI. The optical probe (d) had 2 source (S1 and S2) and 4 detector fibers (D1 to D4). Source-detector separations ranged from 0.5 to 3 cm.

#76741 - $15.00 USD Received 3 November 2006; revised 14 January 2007; accepted 16 January 2007

The DCS probe shown in Fig. 2(d) had two multi-mode source fibers (diameter = 200 μm, length = 12 meter) and four single-mode detector fibers (diameter = 7 μm, length = 12 meter). An optical switch (1*4 Prism, Dicon Fiberoptics Inc., CA) connected with the CW laser source (785 nm) was employed to switch the two source positions consecutively. Four detector fibers were connected to the four APDs. The full-frame-acquisition time for the DCS measurement was 3.4 seconds.

The source-detector separations of the optical probe ranged from 0.5 to 3 cm (see Fig. 2(d)). From diffusion theory, light penetration depth depends on tissue optical properties and source-detector separation. In the previous study we have experimentally demonstrated that signals detected by source-detector pairs with large separations (>2 cm) derived predominately from the muscle layer, provided the thickness of the near-surface layers (skin and adipose) was small [30]. The thickness of the near-surface layer derived from the MRI anatomic images of the present population (5.5 ± 1.0 mm, n = 7, see Table 1) was comparable with that of previous population (5.5 ± 0.4 mm, n = 10) [30]. Thus, in this study muscle flow responses were obtained by averaging data taken with large source-detector separations (i.e. 2.5 and 3 cm).

2.3 Arterial Spin Labeled MRI (ASL-MRI)

ASL-MRI measurements were conducted in a 3.0 Tesla Siemens Trio whole-body MR system. A custom designed dual-tuned proton/phosphorous transmit-receive knee coil (Nova Medical, Inc., Wakefield, MA) was employed. A single-slice version of the continuous ASL (CASL) sequence was utilized for muscle perfusion MRI [45, 46]. The raw image series were separated into label and control pairs and then pair-wise subtracted. The labeling plane was 6 cm proximal to the imaging slice in the axial plane, whereas the inversion plane was placed 6 cm distal to the imaging slice during the control state. Imaging parameters were: single slice of 1 cm thickness, field of view = 22 cm, matrix size = 48 x 64, TR/TE = 4000/13ms, tagging duration = 2 sec. A post labeling delay of 1900 ms was employed based on previous testing [47]. Because the employed cuff occlusion paradigm may cause relatively large dynamic changes in the raw echo-planar image (EPI) series, the pair-wise subtraction between successive label and control acquisitions is susceptible to contamination from the changes in the "static" signals. To minimize this confounding effect, the control image series were first linearly interpolated so that the pair-wise subtraction was carried out using time matched label and control images [48].

In order to eliminate the residual static signal between label and control acquisitions caused by imperfection of the gradient, the polarity of the applied gradient was flipped every pair of label and control acquisitions. Consequently for analysis, two adjacent data points in the subtracted difference perfusion image series were averaged, resulting in an effective temporal resolution of 16 seconds per sample [49]. Flow quantification followed the model in reference 46 (Eq. [1]), assuming blood T_1 = 1.5 sec and a blood-tissue water partition coefficient of 0.9 mL/g.

2.4 Co-registration of optical and ASL-MRI measurements

MRI anatomic images enabled co-registration of DCS and ASL-MRI measurements. For example, the location of DCS probe is determined approximately from the rectangular deformation area due to probe pressure on the tissue surface (see Fig. 2(a), Fig. 2(b) and Fig. 2(c)). For precise localization, a vitamin E pill, positioned at the center of the DCS probe was used to assist in MRI slice selection of the identical calf region (see Fig. 2(a) and Fig. 2(b)). The region of interest (ROI) (see Fig. 2(a) and Fig. 2(c)) underneath the DCS probe was selected for extraction of data from the ASL-MRI measurements. The ROI was selected according to a simulation of the photon path distribution in the homogeneous tissue for a source-detector pair with a large separation (i.e. 3 cm) [30]. The selected ROIs excluded voxels containing large vessels.

#76741 - $15.00 USD Received 3 November 2006; revised 14 January 2007; accepted 16 January 2007

2.5 Characterization of flow responses

The time course of DCS measurements of relative blood flow (rBF) and ASL-MRI measurements of perfusion are presented as measured values ± their error bars. In order to evaluate DCS measurement accuracy we assumed that signal fluctuations measured at rest are due to instrumental and physiological noise [30], and we estimated a percent error from the standard deviation of 20 measurement time-points at rest divided by their mean. The ASL-MRI measurement error was estimated by the standard deviation of measurement time-points *during* cuff-occlusion, since most of the patients were not measured by the ASL-MRI at rest. The measurement error of baseline/cuffed perfusion measured by ASL-MRI is large as a result of the very low blood perfusion which produces a poor signal-noise-ratio [50]. We thus limited the comparison of the two measurements to data taken in the vicinity of the hyperemic peak, that is, excluding DCS/ASL-MRI data with MRI perfusion less than 10 (ml/100g)/min [50].

To characterize flow responses, mean and standard deviation are calculated for peak blood flow (reactive hyperemia) after release of cuff-occlusion, a time constant is calculated from release of cuff-occlusion to peak blood flow (i.e. Time-to-Peak (sec)), and recovery half-time is calculated (i.e. Time-after-Peak (sec)). Figure 3(a) illustrates the definition of these variables. A two-sample t-test was used to identify the differences between DCS and ASL-MRI measurements. Correlations between DCS and ASL-MRI measurements were determined by linear regression analysis. The criterion for significance was $p < 0.05$.

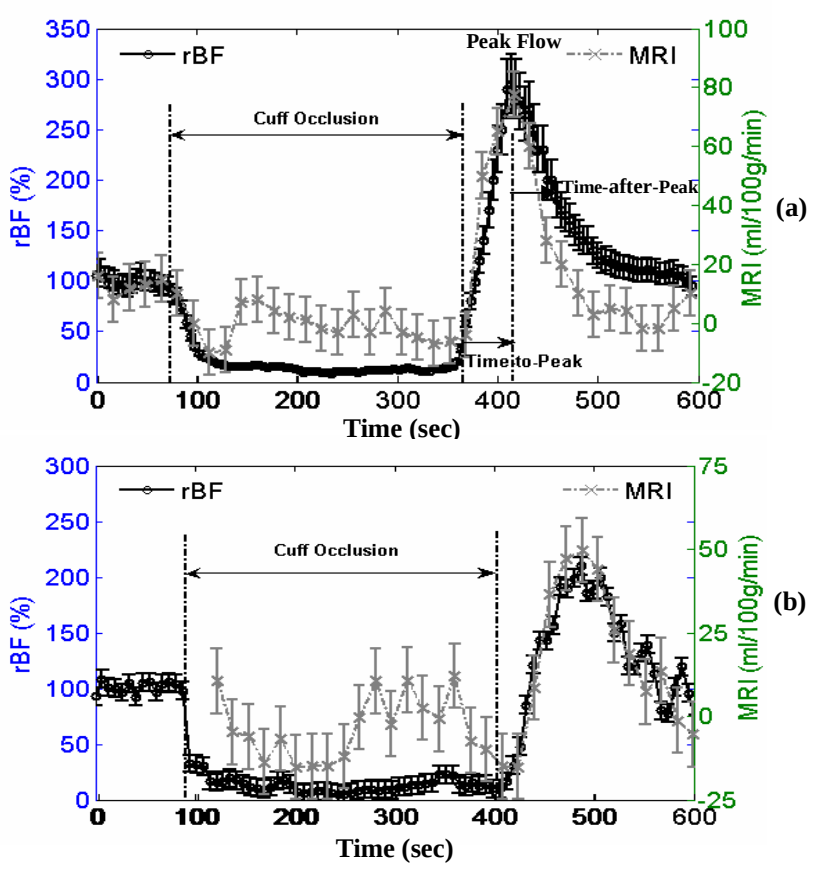

Fig. 3. Time course of the blood flow response from two healthy volunteers (a and b) measured by DCS (dark circles) and ASL-MRI (light crosses) during 5-min cuff occlusion. DCS/MRI measurement error was estimated by the signal variations at rest/during cuff occlusion. Vertical lines indicate beginning and end of the cuff occlusion. Blood flow responses were characterized by peak blood flow, Time-to-Peak (sec), and Time-after-Peak (sec).

#76741 - $15.00 USD Received 3 November 2006; revised 14 January 2007; accepted 16 January 2007

3. Results

3.1 Flow responses

Figure 3 shows the typical dynamic changes in blood flow measured by DCS and ASL-MRI during 5-minute cuff occlusion from two volunteers. The DCS and ASL-MRI blood flow curves exhibited similar dynamic responses in each individual. For the DCS measurement, the rapid increase of cuff pressure induced a significant decrease in blood flow (-91.0 ± 3.2%, n = 7), assigning 100% as the baseline. The typical reactive hyperemic peak blood flow following the release of cuff inflation was 267.0 ± 50.2%. These optical measurement results are in good agreement with previous optical-only observations of healthy volunteers (-90.0 ± 2.4%, 311.4 ± 90.8%, n = 10) [30].

As noted above, the signal-noise-ratio (SNR) of the ASL-MRI method is relatively poor when tissue perfusion is low. For example, muscle blood flow at rest (3-5 (ml/100g)/min [7, 51, 52]) and during cuff occlusion (biological zero flow) are fairly low, and their measurements are accompanied by relatively large error bars in ASL-MRI perfusion responses (see Fig. 3). Occasional "negative flow" ASL-MRI values were also observed during cuff occlusion (see Fig. 3); these arise from raw signal contamination even with the time matched subtraction after interpolation [53] (Note, the ASL signal requires a subtraction of label and control image pairs). For this reason we employed a cuff manipulation paradigm to generate a state of hyperemia. On average, the mean peak ASL-MRI flow after release of cuff occlusion was 68.1 ± 21.2 (ml/100g)/min (n = 7).

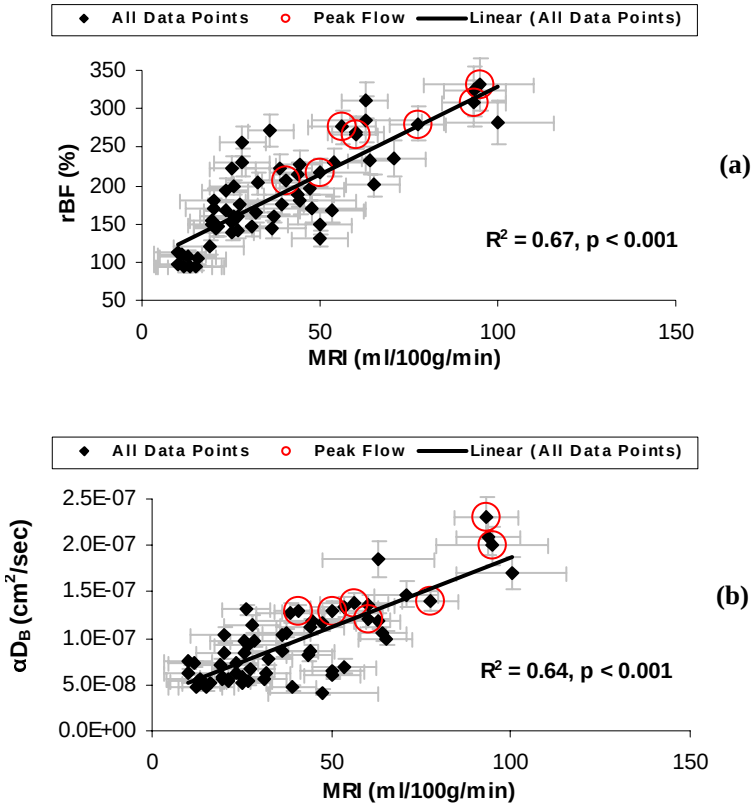

Fig. 4. Correlations between ASL-MRI flow and DCS relative blood flow (a), and DCS flow-index αDB (b). All datasets (solid dots) are obtained by ASL-MRI and DCS at identical time points from 7 subjects, including seven peak flow values (empty circles). Peak flow is defined as the maximum flow value after release of cuff occlusion (see Fig. 3(a)).

#76741 - $15.00 USD Received 3 November 2006; revised 14 January 2007; accepted 16 January 2007

To evaluate the measurement repeatability, three subjects were sequentially measured twice. The variations in peak blood flow between two repeated measurements on three subjects (n = 3) were less than 8% for both DCS and ASL-MRI.

The probe pressure on soft muscle tissues introduced muscle deformation (see Fig. 2) which sometimes affected the muscle blood flow. When wrapping the optical probe, it was found that the mean peak ASL-MRI flow (57.7 ± 21.2 (ml/100g)/min, n = 4) was significantly lower than that without the optical probe (100.2 ± 32.5 (ml/100g)/min, p = 0.03).

3.2 Correlations between optical and ASL-MRI measurements

Figure 4 shows the comparison of muscle blood flow measurements obtained by ASL-MRI and DCS at *identical* time points during 5-minute cuff occlusion from 7 subjects. We compared DCS flow and absolute ASL-MRI perfusion data taken around the peak of the hyperemia after cuff release. Significant linear correlations ($R^2 > 0.60$, $p < 0.001$) between absolute ASL-MRI perfusion and DCS relative blood flow (Fig. 4(a)), and DCS absolute flow-index αD_B (Fig. 4(b)) were found. The peak values of blood flow showed stronger correlations ($R^2 > 0.70$, $p < 0.05$, see Fig. 5) than those obtained from all data points (see Fig. 4). Note also, the DCS relative blood flow (rBF) exhibited a stronger correlation with ASL-MRI perfusion than the absolute DCS flow-index αD_B for all data points and for peak flow (see Fig. 4 and Fig. 5).

In this study we also observed that the ASL-MRI Time-to-Peak (52.6 ± 7.8 sec) and ASL-MRI Time-after-Peak (36.6 ± 7.8 sec) were shorter than the DCS Time-to-Peak (62.2 ± 9.2 sec) and DCS Time-after-Peak (46.4 ± 9.3 sec), respectively. These differences, however, are not significant ($p > 0.08$), and they may be attributed to measurement errors created by the low ASL-MRI temporal resolution (16 seconds).

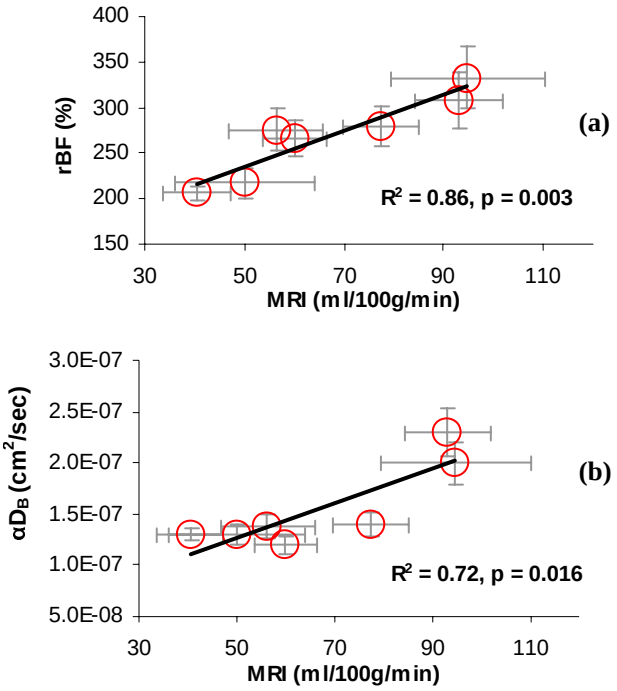

Fig. 5. Correlations between ASL-MRI peak flow and DCS peak relative blood flow (a) and DCS peak flow-index αD_B (b).

#76741 - $15.00 USD Received 3 November 2006; revised 14 January 2007; accepted 16 January 2007

4. Discussion and conclusion

In this study, the absolute DCS flow-index αD_B and its relative change (rBF) were found to be significantly correlated with tissue blood perfusion measured by ASL-MRI; correlation in the latter case was stronger. Uncertainty about the assumed value of the tissue scattering coefficient μ_s' (5 cm^{-1}) can introduce calculation errors in the absolute index αD_B [30]. In principle, however, μ_s' can be concurrently measured using a hybrid instrument [22, 23, 30], thus eliminating this source of error. The variation of the fiber-tissue coupling coefficients during each measurement or between different measurements may also create errors in estimation of αD_B. These calculation and measurement errors are largely normalized out in the rBF data [30]. Therefore, it is not surprising to observe the stronger correlations of ASL-MRI with relative blood flow (rBF).

In our observation range (i.e. for ASL-MRI perfusion >10 (ml/100g)/min) the absolute DCS measurement (αD_B), in units of cm^2/s, was found to be linearly proportional to the ASL-MRI measurement, in units of (ml/100g)/min (see Fig. 4(b)). These observations suggest that absolute DCS data may be regarded as an index of blood flow, and the slope of the best-fit line in Fig. 4(b), i.e. $[1.5 \pm 0.15] \times 10^{-9}$ $(cm^2/s)/(ml/100g)/min$, can be used for calibration of DCS data (αD_B). Over a narrow observation range (i.e. for ASL-MRI perfusion > 40 (ml/100g)/min), the linear correlation between the two measurements became stronger (see Fig, 5(b)). This was likely due to the smaller percentage error of the ASL-MRI measurements at higher flow levels. The slope of this best-fit line, i.e. $[1.7 \pm 0.47] \times 10^{-9}$ $(cm^2/s)/(ml/100g)/min$, can be used for better calibration of DCS flow-index in the higher flow observation range. Conceptually, some limitations are apparent. The factor α is a measure of the ratio of moving scatterers (i.e. blood cells) to static scatterers in tissue. This factor could vary with tissue-type, subject hematocrit, etc. In addition, the microscopic nature of the effective diffusion coefficient, D_B, is not well understood, and it will certainly depend on the spatial distribution and relative volume fraction of arterioles, venules and capillaries of the observed tissue microvasculature. In principle some of these factors (e.g. hematocrit) can be concurrently measured and corresponding corrections applied, but, for the long-term, it is important to catalogue this slope across tissue type and over large sample sizes. After such a study, it should be possible to derive calibration coefficients specific to particular organs, tissues and disease.

On the other hand, measurements of relative changes of blood flow are valuable. Such changes have already been shown to be useful in a variety of clinical contexts, for example diagnosis of cancer [28, 29, 54, 55], evaluation of muscle vascular disease [30], and assessment of therapeutic response [26, 27, 29, 56, 57]. Some of these measurements monitored relative blood flow changes continually for several hours/days/weeks after radiation treatment [26, 29], and information obtained from these studies was useful for estimation of treatment effect. Taken together, our results indicate that relative blood flow (e.g., rBF measured by DCS) holds potential for the purpose of longitudinal monitoring of tissue physiological status, and we have established in this paper that rBF is closely related to blood flow measured by ASL-MRI.

The concurrent measurement also provided an opportunity to evaluate the influence of probe pressure on muscle blood flow. The pressure created by the optical probe affected blood flow significantly, but was not an issue for this study since the increased pressure affected DCS and ASL-MRI measurements to the same degree. In future all-optical measurements, it will be desirable to tape (without wrapping) a 'light-material' probe on calf to reduce pressure or to measure pressure directly using embedded pressure sensors in order to insure repeatability.

MRI provides anatomic information for accurate co-registration of optical and ASL-MRI measurements. Such information (e.g. the thickness of tissue layers) is useful for more precise quantification of DCS signals, including blood flow heterogeneity in different tissue layers (e.g., skin, adipose, muscle). Even at large source-detector separations there always exists some contribution to the DCS signal from overlaying tissues (skin and adipose). The

#76741 - $15.00 USD Received 3 November 2006; revised 14 January 2007; accepted 16 January 2007

ASL-MRI/Optical approach takes a first step towards understanding these effects, but will require more source-detector coverage and multi-layer modeling for progress.

Finally, we revisit the claim that near-infrared diffuse correlation spectroscopy (DCS) and arterial spin labeled perfusion MRI (ASL-MRI) both measure microvascular flow. Diffuse optical techniques are known to be sensitive to smaller vessels such as arterioles, capillaries, and venules in tissue [58]; the absorption in large vessels is so large that photons are absorbed before penetrating through these structures. ASL-MRI also measures blood flow through tissue microvasculature, but transit related effects can give rise to intravascular signals from large vessels in ASL-MRI perfusion images, thereby increasing the vascular/arterial weighting in the measured ASL-MRI signal. In order to determine the optimal parameters for ASL-MRI in human muscles, multiple ASL-MRI measurements at a series of delay times (900, 1200, 1500, 1900 ms) were carried out in a separate pilot study [47], and a long delay of 1900 ms was chosen for the present study. This choice weighted the ASL-MRI signal more towards the microvasculature. Furthermore, the reported ASL-MRI perfusion values were extracted from ROIs that were manually drawn to *exclude* voxels containing large vessels. Therefore, we believe the two techniques in this study compare signals from essentially the same tissue microvasculature.

To conclude, we have shown that diffuse correlation spectroscopy (DCS) and ASL-MRI quantify the same temporal dynamics of tissue microvascular flow. DCS provides a rapid, non-invasive, portable and quantitative bedside tool for assessment of muscle blood flow. Both DCS relative blood flow (rBF) and absolute flow-index (αD_B) are strongly correlated with the ASL-MRI perfusion. Those findings represent a first step toward calibration of diffuse optical flow-indices.

Acknowledgments

We acknowledge support from NIH grants HL-083225, HL-75649, HL-077699, and AHA 0665446U. We are also grateful for assistance from J.M. Murphy with subject recruitment and technology, and for useful discussions with E.R. Mohler III and G. Lech.

#76741 - $15.00 USD Received 3 November 2006; revised 14 January 2007; accepted 16 January 2007